Available online at www.sciencedirect.com
ScienceDirect
Trans. Nonferrous Met. Soc. China 26(2016) 2532−2541
Transactions of Nonferrous Metals Society of China
www.tnmsc.cn

Effect of homogenization annealing on microstructure, composition and mechanical properties of 7050/6009 bimetal slab

Guang-yuan YAN[1], Feng MAO[1], Fei CHEN[1], Zhi-qiang CAO[2], Tong-min WANG[1]

1. Key Laboratory of Materials Modification by Laser, Ion, and Electron Beams, Ministry of Education, School of Materials Science and Engineering, Dalian University of Technology, Dalian 116024, China;
2. Laboratory of Special Processing of Raw Materials, Dalian University of Technology, Dalian 116024, China

Received 9 October 2015; accepted 13 June 2016

Abstract: Homogenization annealing of the 7050/6009 bimetal slab prepared by direct-chill casting was investigated and its effects on microstructural evolution, composition distribution and mechanical properties in the interfacial region of the bimetal were studied. The results show that the optimized homogenization annealing process was 460 °C for 24 h. After homogenization annealing, the Zn-rich phases and $Al_{15}(FeMn)_3Si_2$ phases were precipitated at the interface of the bimetal. The diffusion layer thickness of homogenized bimetal increased by 30 μm from 440 to 480 °C for 24 h, while it increased by 280 μm from 12 to 36 h at 460 °C. The Vickers hardnesses at 6009 alloy side and interface of the bimetal decreased after homogenized annealing and grain coarsening was considered as the dominating softening mechanism. The hardness variation at 7050 alloy side was complicated due to the combined action of solution strengthening, dispersion strengthening and dissolution of reinforced phases.

Key words: bimetal slab; homogenization annealing; microstructure; diffusion layer; mechanical properties

1 Introduction

The 7050 alloy is considered as an ideal material for preparing aircraft skin due to its high specific strength [1−4]. The 6009 alloy has superior corrosion resistance and good formability, and is widely applied in automobile plates [5−9]. The 7050/6009 bimetal slab can be prepared by direct-chill (DC) casting with a superior combination of high strength and superior corrosion resistance as well as good formability, so as to meet the requirements of mass reduction and safety improvement in automobiles and airplane industries. Generally, bulky precipitated phases at grain boundaries of 7050 alloy deteriorate service performance and limit the range of applicable process parameters during subsequent hot deformation [10]. It is important to directly carry out a homogenization heat treatment after casting before processing to get good working qualities and service performance.

Recently, many works on homogenization heat treatment have been carried out on Al−Zn−Mg−Cu alloy and Al−Mg−Si alloy systems. The effect of homogenization treatment on microstructure and mechanical properties of DC cast 7x50 aluminum alloy was reported [11]. The effects of homogenization treatment on microstructural changes of AA7075 and 7049 alloys were studied [12,13]. LI and STARINK [14] and FAN et al [15] have shown the evolution of microstructure in an Al−Zn−Mg−Cu alloy during homogenization. DENG et al [16] and HE et al [17] studied the evolution of precipitated phase in 7xxx aluminum alloy during homogenization. Besides, the nature of $T(Al_2Mg_3Zn_3)$ and $S(Al_2CuMg)$ phases present in as-cast and annealed 7055 aluminum alloy was investigated [18]. On the other hand, the effects of homogenization conditions on microstructure and mechanical properties of Al−Mg−Si alloys have been the subject of several studies in recent years [19−23]. MARGARITA et al [24] studied the effect of long-term stabilization of TRC AA6016 sheets processed with and without homogenization with the main objective of comparing the properties of TRC and DC materials.

Although such researches have been reported on the evolution of microstructure and precipitated phase during homogenization in the case of Al−Zn−Mg−Cu alloy and

Foundation item: Projects (51375070, 51574058) supported by the National Natural Science Foundation of China
Corresponding author: Zhi-qiang CAO; Tel: +86-411-84706169; Fax: +86-411-84706169; E-mail: caozq@dlut.edu.cn
DOI: 10.1016/S1003-6326(16)64379-0

Al−Mg−Si alloy systems, the information concerning the effect of homogenization annealing on 7050/6009 bimetal slab featuring these two alloys' characteristics is still rarely seen in literatures. It is important to investigate the evolution of microstructure, composition and mechanical properties of 7050/6009 bimetal slab during homogenization annealing and to develop an optimal homogenizing annealing process for the subsequent processing in actual industrial application.

2 Experimental

The experimental materials 7050 alloy and 6009 alloy were prepared separately by melting the commercial pure aluminum, zinc, copper, magnesium, manganese, crystalline silicon and Al−4%Zr master alloy at appropriate ratios in their respective pot resistance furnaces. The 7050/6009 bimetal slab (130 mm × 120 mm × 100 mm) was prepared by a direct-chill (DC) casting process. The chemical compositions of the 6009 alloy and 7050 alloy are given in Table 1. Cubic test samples with dimensions of 5 mm × 10 mm × 20 mm were cut from the center of the as-cast 7050/6009 bimetal slab by wire-electrode cutting. Homogenization annealing processes were performed on these cubic samples at 480, 460, 440 °C for 24 h and 460 °C for 36, 12 h, respectively.

Table 1 Chemical compositions of experimental alloys (mass fraction, %)

Alloy	Zn	Cu	Mg	Si	Fe
7050	6.533	2.273	2.285	0.056	0.109
6009	−	−	0.603	0.955	0.131

Alloy	Zr	Mn	Cr	Al
7050	0.095	0.0036	0.026	Bal.
6009	−	0.003	0.020	Bal.

The as-cast and homogenizing annealed samples were polished and etched with Keller's reagent (1% HF + 1.5% HCl + 2.5% HNO_3 + 95% distilled water, volume fraction), then the microstructure was observed by optical microscope and scanning electron microscope (SEM, Zeiss supra 55) equipped with energy dispersive spectrometer (EDS). The elements distributions in the interfacial region of the bimetal samples were analyzed by electron microprobe (EPMA−1600) operated at 15 kV. A Vickers hardness test was conducted with a load of 50 g for 15 s.

3 Results and discussion

3.1 Microstructure of homogenized bimetal

Figure 1 shows the microstructure in the interfacial region of 6009/7050 bimetal after different homogenization treatments. The two-layer structure in as-cast state was still maintained after homogenizing annealing. It can be seen from Figs. 1(a)−(d) that the content of net structure of 7050 side decreased gradually with the homogenization temperature increasing. When the temperature increased to 480 °C, the net structure of 7050 side mainly faded away, as shown in Fig. 1(d). However, the microstructures of 6009 side and interface showed no significant changes. The microstructure of the bimetal homogenized at 460 °C for different time such as 12, 24 and 36 h are shown in Figs. 1(e), (c) and (f), respectively. It is found that with the homogenization time increasing from 12 to 36 h, the content of net structure of 7050 side decreased significantly, but there was little residual second phase after 36 h homogenization. Meanwhile, no significant changes were found in the microstructures of 6009 side and interface of the bimetal, because there was no coarse precipitation phase forming due to few content of the solute elements at 6009 alloy side and interface of the bimetal.

High magnification SEM images of the interface of 6009/7050 bimetal homogenized at different temperatures for different time are shown in Fig. 2. The results indicate that the second-phase particles are precipitated in α(Al) at the interface of the bimetal during homogenization treatment. These particles, generally exhibiting a bimodal size distribution, consisted of large and fine particles. Large particles were mainly rodlike phases formed from the dissolution of net structure at 7050 alloy side due to diffusion of elements from 7050 alloy side to interface, while finer particles were mainly finer granular phase formed due to diffusion of elements from 6009 alloy side to interface of the bimetal. With increasing homogenization temperature (Figs. 2(b)−(d)) and homogenization time (Figs. 2(e), (c) and (f)), the sizes of rodlike phases and granular phases became slightly larger. Higher homogenization temperature could increase the interface energy, which can promote the growth of rodlike phases and granular phases. It is found that the rodlike phases are Zn-rich phases and granular phases are $Al_{15}(FeMn)_3Si_2$ phases.

Figure 3 shows the high magnification SEM images of the 7050 alloy side of 6009/7050 bimetal homogenized by different homogenization treatments. According to the EPMA results, the composition of skeletal eutectic structure at the grain boundary of 7050 side for the as-cast bimetal slab is 23.467 Zn, 24.856 Cu, 13.450 Mg and 38.127 Al (mass fraction, %), which is in accordance with the α(Al) + T(AlZnMgCu) eutectic structure. Besides, CONG et al [11] also found $MgZn_2$, with a small amount of Al_7Cu_2Fe and Al_3Zr in the as-cast 7x50 alloy. It can be seen that with increasing

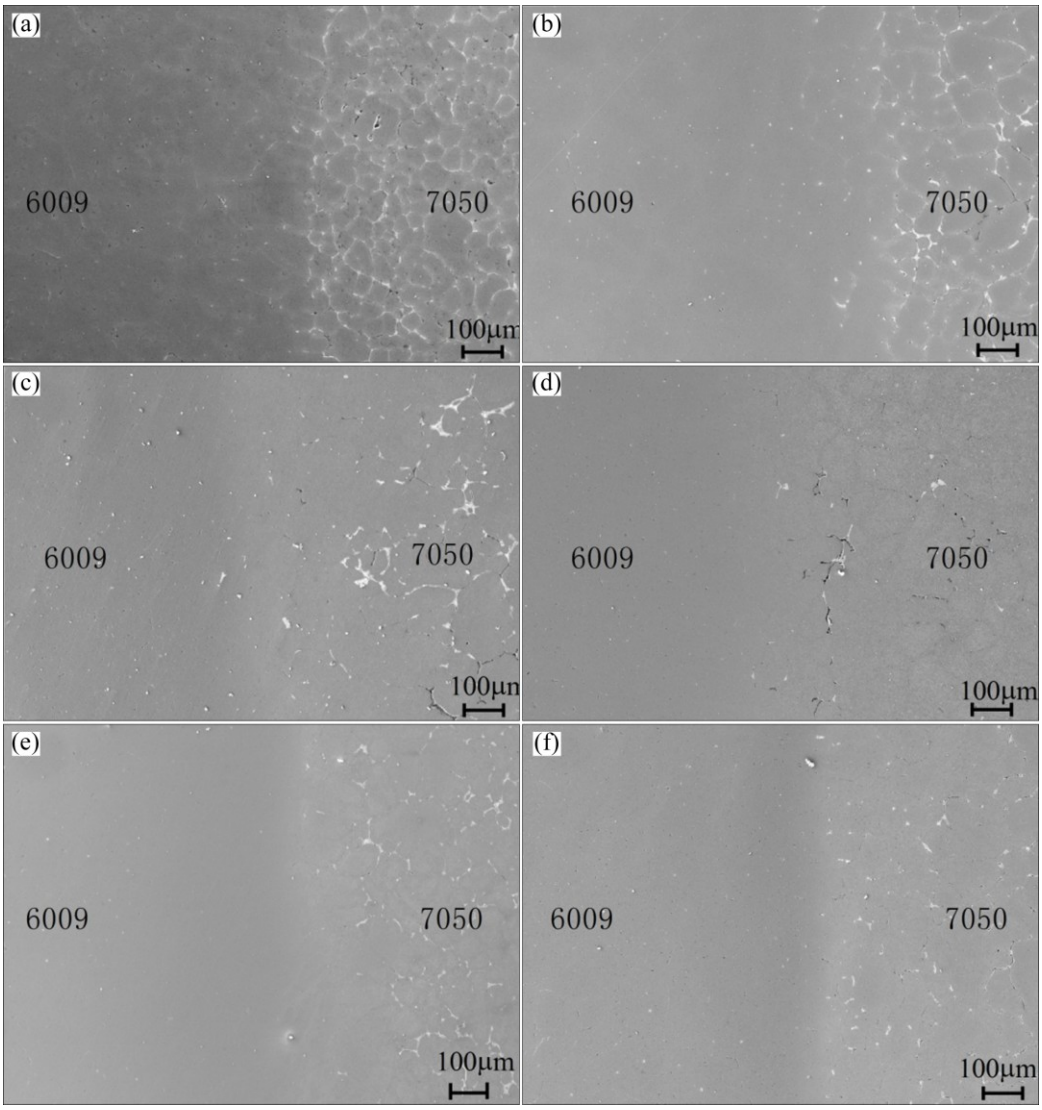

Fig. 1 Secondary electron SEM images in interfacial region of 6009/7050 bimetal homogenized at different temperatures for different time: (a) As-cast; (b) 440 °C, 24 h; (c) 460 °C, 24 h; (d) 480 °C, 24 h; (e) 460 °C, 12 h; (f) 460 °C, 36 h

homogenization temperature, the fraction of α(Al) + T(AlZnMgCu) eutectic structure distributed at the grain boundary decreased and a significant fraction of coarse intermetallic phases remained undissolved at the grain boundaries after homogenization. The EPMA analysis reveals that these intermetallic phases mainly include two kinds of phases: one's composition is 37.554 Al, 45.5 Cu and 16.884 Mg (mass fraction, %), which is in accordance with S-phase (Al_2CuMg); the other is considered as Al_7Cu_2Fe containing 58.443 Al and 41.511 Cu (mass fraction, %). The rounded S-phase and insoluble constituent phase Al_7Cu_2Fe were also identified by CONG et al [11] and ROBSON [25]. In addition, there are more and more apparent rod-like phases precipitated within the grains. EDX measurements show that these rod-like particles are rich in zinc, and therefore correspond to Mg(Zn_2AlCu) M-phase. The rod-like M-phase had also been observed in 7050 alloy slow cooling to 400 °C followed by quenching [25] and 7050 alloy slow quenching from solutionization [26]. Besides, the size of rodlike Zn-rich phases increased slightly with the homogenization temperature increasing from 440 to 480 °C, and this slight increase in size of Zn-rich phases could be ascribed to the augment of interface energy caused by increasing temperature. These rodlike Zn-rich particles within the grains firstly gathered nearby the residual second phases at the grain boundary (Fig. 3(b)), then towards the grain matrix (Fig. 3(c)). When the homogenization temperature was increased to 480 °C, the Zn-rich phases distributed uniformly within the grains and skeletal eutectic structure disappeared, as shown in Fig. 3(d). Many fine precipitated phases precipitated within the grains nearby the residual second phase at the grain boundary when homogenization time is 12 h at 460 °C, as shown in Fig. 3(e). When the time increased to 24 h (Fig. 3(c)), it is observed that the

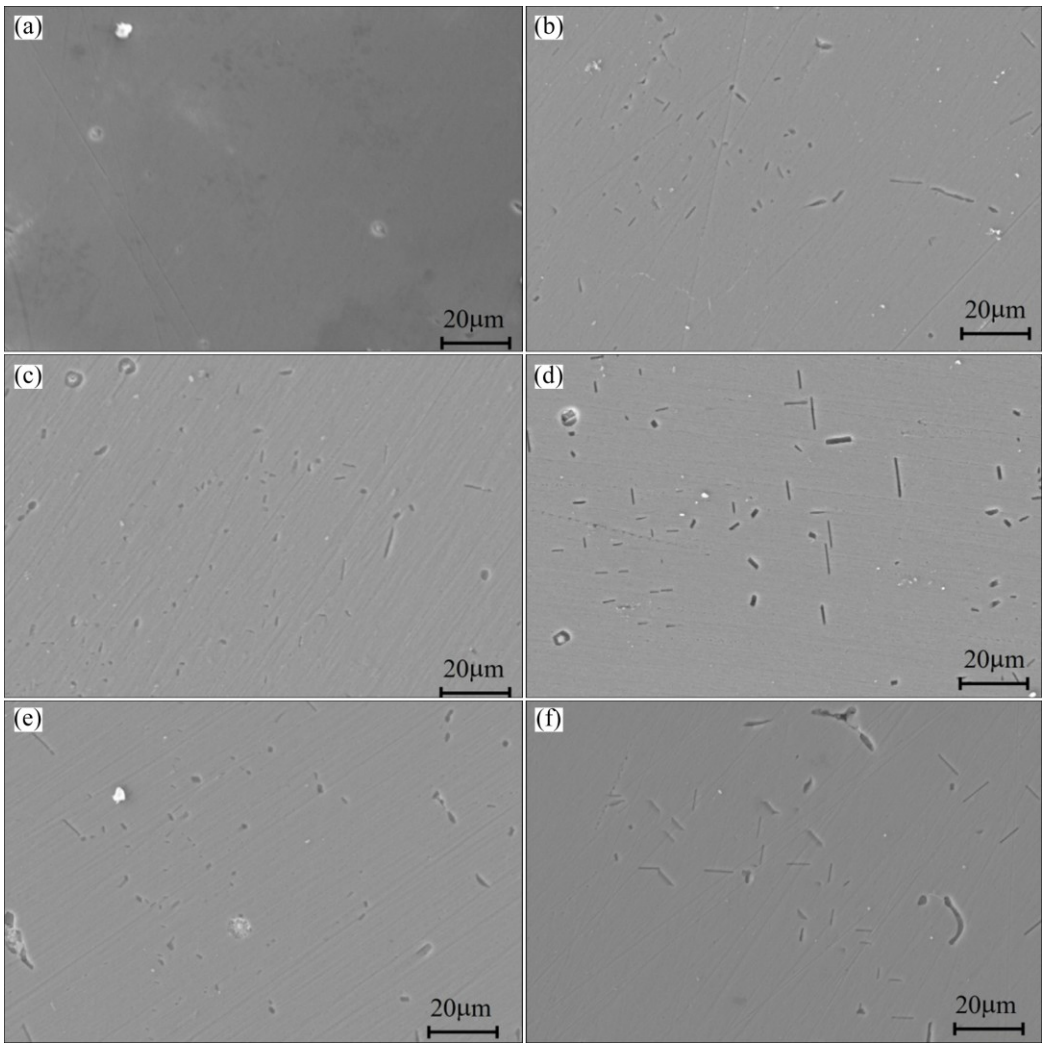

Fig. 2 Secondary electron SEM images of high magnification at interface of 6009/7050 bimetal homogenized at different temperatures for different time: (a) As-cast; (b) 440 °C, 24 h; (c) 460 °C, 24 h; (d) 480 °C, 24 h; (e) 460 °C, 12 h; (f) 460 °C, 36 h

volume fraction of precipitated phase increased significantly and these precipitated phases distributed uniformly within the grains when homogenization time increased to 36 h. Furthermore, with the homogenization time increased from 12 to 36 h, these precipitated phases grew up into rod-like Zn-rich phases. The precipitation of Zn-rich phases firstly nearby the grain boundary may be attributed to the supersaturation caused by the dissolution of α(Al) + T(AlZnMgCu) eutectic phases and non-equilibrium phases at grain boundary. The area of Zn-rich phases then spread into grain inner due to diffusion of alloy elements. The results support the as-mentioned case that the rod-like phases at the interface of the bimetal are precipitated from the dissolution of α(Al) + T(AlZnMgCu) eutectic phases at 7050 alloy side due to diffusion of elements from 7050 side to the interface of the bimetal.

High magnification SEM images of 6009 side of 6009/7050 bimetal homogenized under different conditions are shown in Fig. 4. The results indicate that the fine granular phases are formed in the matrix during the homogenization annealing compared to the as-cast condition. The fine granular phases are considered as $Al_{15}(FeMn)_3Si_2$ because YAN et al [19] found that the remaining phases were α(Al) and $Al_{15}(FeMn)_3Si_2$ for Al−0.66Mg−0.85Si alloy after homogenization treatment. The average size of granular $Al_{15}(FeMn)_3Si_2$ phases increased when homogenization temperature increased from 440 to 460 °C, while the average size of granular phases decreased when homogenization temperature increased from 460 to 480 °C. The main reason why the size of precipitated phases can increase may be that the growth speed of precipitate phases increased when homogenization temperature increased from 440 to 460 °C. While this decreased size may be on account of the sharp increase of nucleation rate caused by higher homogenization temperature from 460 to 480 °C, which was conducive to precipitation of finer $Al_{15}(FeMn)_3Si_2$ phases. The results are in accordance with the as-mentioned case that the fine granular phases in the

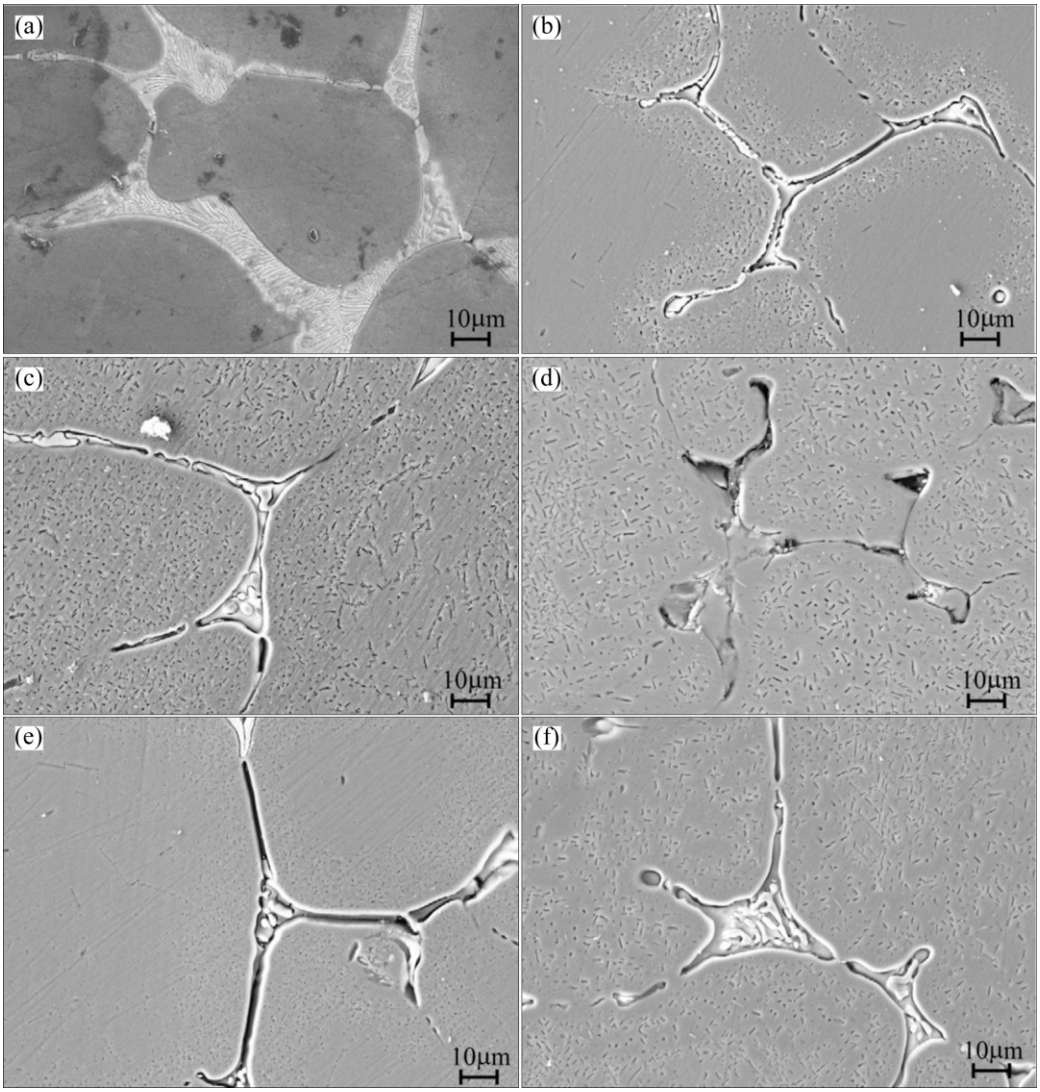

Fig. 3 Secondary electron SEM images of high magnification at 7050 side of 6009/7050 bimetal homogenized at different temperatures for different time: (a) As-cast; (b) 440 °C, 24 h; (c) 460 °C, 24 h; (d) 480 °C, 24 h; (e) 460 °C, 12 h; (f) 460 °C, 36 h

interface of bimetal are precipitated due to the diffusion of elements from 6009 alloy side to interface.

3.2 Composition variations of homogenized bimetal

Figure 5 shows the composition variations of the Zn, Cu, Mg and Si elements in the interfacial region of the bimetal after different homogenization treatments. The result reveals that the bimetal slab retains the layered characteristics of as-cast. In present study, the thickness of diffusion layer is defined as the diffusion distance of Zn element across the interface. It can be seen that the diffusion layer thickness of the bimetal became larger significantly and the composition variation curves of the Zn, Cu, Mg and Si elements became smoother after homogenization annealing, compared to as-cast state. The smoother composition variation curves indicated that the bimetal achieved more uniform elements distribution after homogenization annealing. The composition variation curves of the Zn, Cu, Mg and Si elements became smoother with the homogenization temperature increasing from 440 to 480 °C, as shown in Figs. 5(b)−(e). Because the solute diffusion coefficients increased with increasing the diffusion temperature so as to achieve more uniform elements distribution at the same diffusion time. With homogenization time increasing from 12 to 36 h, the smoother composition distribution curves were also found in Figs. 5(e), (c) and (f), which were attributed to the sufficient diffusion time.

Moreover, the 7050 alloy is enriched with Zn, Cu, Mg elements, while the 6009 alloy mainly contains Mg and Si elements. As concentrations difference of these elements existed between the two alloys, according to the Fick's law, the interdiffusion took place during homogenization annealing, i.e., Zn, Cu, Mg atoms diffused from the 7050 alloy side to the 6009 alloy side, while Si atoms moved in the opposite direction during

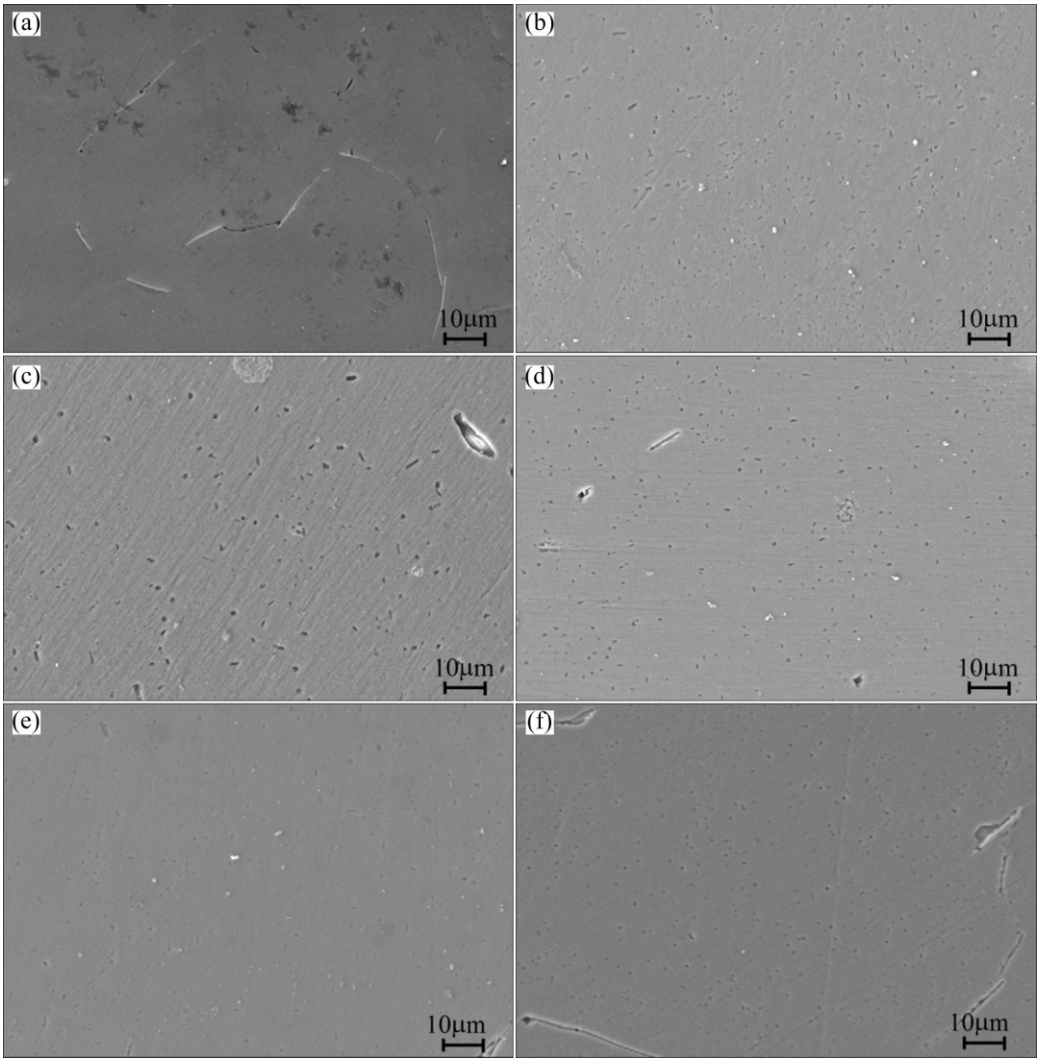

Fig. 4 Secondary electron SEM images in high magnification at 6009 side of 6009/7050 bimetal homogenized at different temperatures for different time: (a) As-cast; (b) 440 °C, 24 h; (c) 460 °C, 24 h; (d) 480 °C, 24 h; (e) 460 °C, 12 h; (f) 460 °C, 36 h

homogenization treatment. This implies that solute distribution in the diffusion layer is inevitable. The research concentrated on the diffusion behavior of alloying elements for 2024/3003 gradient composite during heat treatment was reported [27]. WANG et al [28] studied the diffusion behavior of alloying elements in the interfacial region of 8090/3003 bimetal slab during T6 treatment. Generally, there are at least three kinds of diffusion behaviors that can take place in the interfacial region during heat treatment, i.e., long distance diffusion across the entire interfacial region, short distance diffusion for homogenization of dendrite and short distance diffusion for precipitation in α(Al).

The diffusion layer thicknesses of the bimetal after different homogenization treatments are shown in Fig. 6. In this work, the diffusion distances can be represented by the difference values between diffusion layer thicknesses under different homogenization conditions. With the homogenization temperature increasing from 440 to 480 °C, the diffusion layer thickness of bimetal gained a slight increase from 700 to 730 μm, and the corresponding diffusion distance is 30 μm, as shown in Fig. 6(a). The slight increase in diffusion layer thickness was attributed to the slight augment in diffusion rate of Zn element with increasing diffusion temperature from 440 to 480 °C. However, the diffusion layer thickness of bimetal increased dramatically from 520 to 800 μm with homogenization time increasing from 12 h to 36 h at 460 °C, which resulted from the further diffusion distance (280 μm) for Zn element with increasing diffusion time from 12 to 36 h. The increased diffusion layer thickness also indicates that the long distance diffusion mostly ceases when the bimetal is subjected to homogenization at 460 °C, which is accompanied by short distance diffusion.

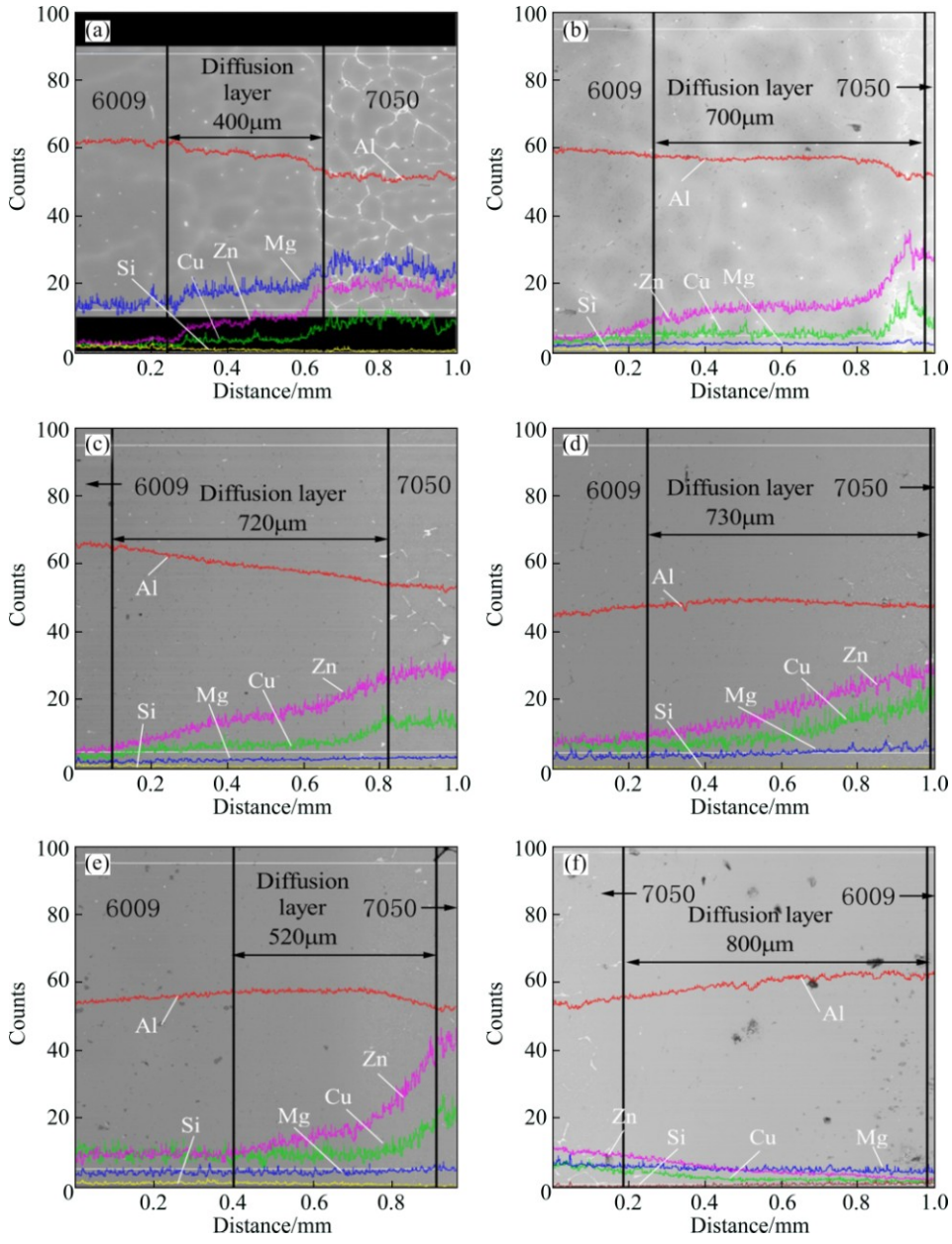

Fig. 5 EPMA line analysis in interfacial region of bimetal at different homogenization treatments: (a) As-cast; (b) 440 °C, 24 h; (c) 460 °C, 24 h; (d) 480 °C, 24 h; (e) 460 °C, 12 h; (f) 460 °C, 36 h

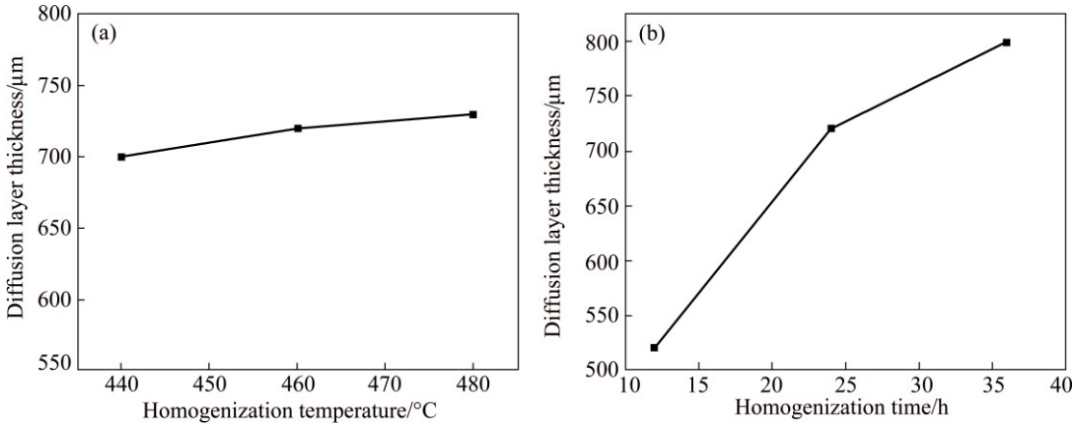

Fig. 6 Variation of diffusion layer thickness of bimetal after different homogenization temperatures for 24 h (a) and homogenization time at 460 °C (b)

3.3 Mechanical properties of homogenized bimetal

The Vickers hardnesses across the interface of the bimetal were measured after different homogenization treatments, and the results are presented in Fig. 7. The layered distribution of Vickers hardness in the interfacial region maintained after homogenizing annealing. The influence of homogenization temperature on hardness of the bimetal is shown in Fig. 7(a). At the 7050 alloy side, the hardness increased with increasing homogenization temperature at the beginning and reached a peak when the homogenization temperature was 460 °C. Then, the hardness decreased after the homogenization temperature continued to increase. During homogenizing annealing, massive reinforcing phases such as $T(Al_2Mg_3Zn_3)$ and $MgZn_2$ dissolved, then Zn, Mg and Cu atoms dissolved into α(Al) and solid solution formed. Besides, nanometer-sized dispersoids such as Al_3Zr, Cr-containing dispersoids may precipitate in α(Al) matrix after homogenizing annealing [29,30]. The dominating strengthening mechanism of 7050 alloy may be solution strengthening and dispersion strengthening, while the dissolution of reinforced phases was considered as the dominating softening mechanism. When the homogenization temperature was 460 °C, the influence of solution strengthening and dispersion strengthening on 7050 alloy was more obvious than that of dissolution of reinforced phases, so the Vickers hardness reached the peak at 460 °C for 24 h. At the 6009 alloy side, the hardness decreased remarkably compared to the as-cast state, after the bimetal samples were homogenized for 24 h. Generally, the grains of metallic materials will grow up after homogenization treatment for reducing gross interface energy of grain boundaries. Furthermore, after homogenization treatment, the grains of Al−0.66Mg− 0.85Si alloy were observed to grow up obviously by electro-polished and anode coated and Mg_2Si, Si phases were dissolved into matrix [19]. Therefore, it is reasonable to infer that the grains of 6009 alloy grow up after homogenization treatments. The dominating softening mechanism of 6009 alloy may be grain coarsening, which weakens the dislocation reinforcement at the grain boundary, resulting in the lower hardness. Besides, the dissolution of reinforced phases Mg_2Si, Si phases could also cause lower hardness. The hardness profiles at 6009 alloy side were fluctuant drastically after the bimetal was subjected to homogenization at 440 °C for 24 h. This fluctuation was attributed to nonuniform microstructure after homogenizing annealing. Then, the average hardness at 6009 alloy side increased from HV 35 to HV 45 with the homogenization temperature increasing from 460 to 480 °C, as shown in Figs. 4(c) and (d). The improved hardness resulted from enhanced dispersion strengthening effect on account of finer $Al_{15}(FeMn)_3Si_2$ phase in the 6009 alloy matrix. Interestingly, the Vickers hardness of interface decreased slightly after homogenizing annealing. Furthermore, with homogenization temperature increasing from 440 to 480 °C, the hardness of interface also decreased. These decreased hardnesses imply that the interface of the 6009/7050 bimetal slab can be softened via homogenizing annealing. The grain size at the interface became bigger after homogenizing annealing, which weakens dislocation strengthening effect at the grain boundary, so as to decrease hardness.

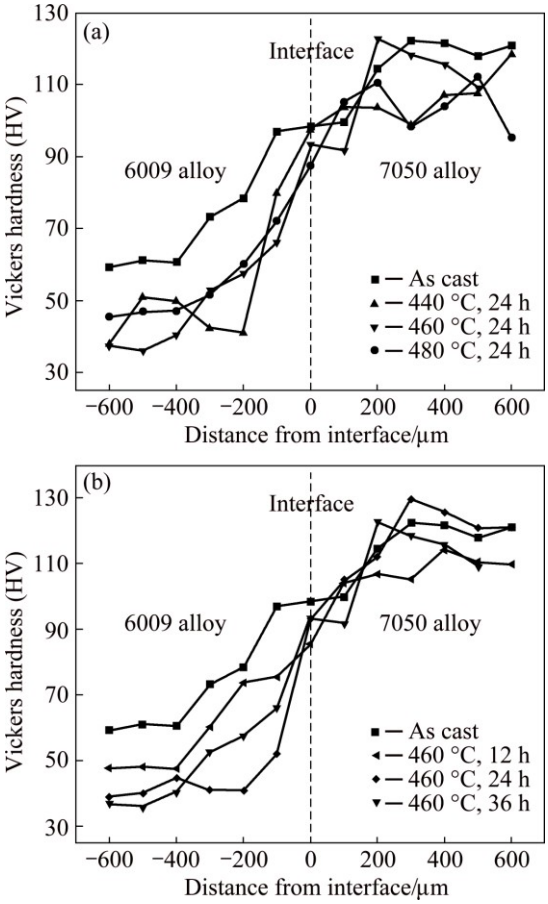

Fig. 7 Vickers hardness across interface of bimetal after different homogenization temperatures for 24 h (a) and homogenization time at 460 °C (b)

Figure 7(b) shows the Vickers hardness distribution across the interface of the 6009/7050 bimetal after homogenizing annealing at 460 °C for 12, 24 and 36 h, respectively. At the 7050 alloy side, the results indicate that the hardness showed no obvious change compared to that of the as-cast state and increased with the increasing homogenization time. A large amount of second phases at the grain boundary dissolved into the matrix so as to promote solution strengthening. Furthermore, dispersion strengthening on the 7050 alloy side was reinforced because more dispersoids formed in α(Al) when homogenization time was prolonged. At the 6009 alloy

side, however, the hardness variation caused by homogenization time was not the same as that on 7050 alloy side. The hardness decreased significantly to HV 47 after the bimetal was subjected to homogenizing annealing for 12 h at 460 °C, compared to the as-cast state. When the homogenization time increased from 12 to 24 h, the hardness decreased from HV 47 to HV 35. While the hardness had no obvious change when homogenization time was prolonged from 24 to 36 h. With prolonging homogenization time, the grains at 6009 alloy side grew up, which weakened observably dislocations strengthening effect in grain boundary so that the hardness decreased. Dispersion strengthening, caused by fine granular phases formed in the matrix, was limited because of a small quantity of Mg and Si elements in 6009 alloy. At the interface of the bimetal, the hardness decreased after homogenizing annealing and increased slightly when prolonging homogenization time from 12 to 24 h and 36 h. This increased hardness was attributed to solution strengthening caused by the interdiffusion of solute elements between 6009 and 7050 alloy, and dispersion strengthening resulting from Zn-rich phases and $Al_{15}(FeMn)_3Si_2$ phases formed in α(Al).

From the above experimental results, the optimized homogenizing annealing process of the 7050/6009 bimetal slab can be determined as 460 °C for 24 h, at which the bimetal shows more uniform microstructure and hardness distribution.

4 Conclusions

1) The optimized homogenization annealing process of the 7050/6009 bimetal slab was 460 °C for 24 h.

2) After homogenization annealing, rodlike Zn-rich phases and granular $Al_{15}(FeMn)_3Si_2$ phases precipitated in α(Al) at the interface of the 7050/6009 bimetal. Moreover, Zn-rich phases and $Al_{15}(FeMn)_3Si_2$ phases precipitated in α(Al) at 7050 alloy side and 6009 alloy side, respectively.

3) With the homogenization temperature increasing from 440 to 480 °C, the diffusion layer thickness of the bimetal gained a slight increase from 700 to 730 μm because of slight augment in diffusion rates of Zn element. However, the diffusion layer thickness increased dramatically from 520 to 800 μm with homogenization time increasing from 12 to 36 h at 460 °C, which indicated that the long distance diffusion mostly ceased when the bimetal was subjected to homogenization at 460 °C.

4) The Vickers hardness at 6009 alloy side and interface decreased after homogenization annealing and the dominating softening mechanism may be grain coarsening. The hardness variation at 7050 alloy side was complicated due to the combined action of solution strengthening, dispersion strengthening and dissolution of reinforced phases.

References

[1] ZOU Liang, PAN Qing-lin, HE Yun-bin, WANG Chang-zhen, LIANG Wen-jie. Effect of minor Sc and Zr addition on microstructures and mechanical properties of Al−Zn−Mg−Cu alloys [J]. Transactions of Nonferrous Metals Society of China, 2007, 17: 340−345.

[2] AL-RUBAIEA K S, del GRANDEA M A, TRAVESSAA D N, CARDOSO K R. Effect of pre-strain on the fatigue life of 7050-T7451 aluminium alloy [J]. Materials Science and Engineering A, 2007, 464: 141−150.

[3] WILLIAMS J C, STARKE E A Jr. Progress in structural materials for aerospace systems [J]. Acta Materialia, 2003, 51: 5775−5799.

[4] FENG Chun, SHOU Wen-bin, LIU Hui-qun, YI Dan-qing, FENG Yao-rong. Microstructure and mechanical properties of high strength Al−Zn−Mg−Cu alloys used for oil drill pipes [J]. Transactions of Nonferrous Metals Society of China, 2015, 25: 3515−3522.

[5] LI Yuan-yuan, ZHENG Xiao-ping, ZHANG Wei-wei, LUO Zong-qiang. Effect of deformation temperature on microstructure and properties of 7075/6009 alloy [J]. Transactions of Nonferrous Metals Society of China, 2009, 19: 1037−1043.

[6] SAKURAI T. The latest trends in aluminum alloy sheets for automotive body panels [J]. Kobelco Technology Review, 2008, 28: 22−28.

[7] KOLAR M, PEDERSEN K O, GULBRANDSEN-DAHL S, MARTHINSEN K. Combined effect of deformation and artificial aging on mechanical properties of Al−Mg−Si alloy [J]. Transactions of Nonferrous Metals Society of China, 2012, 22: 1824−1830.

[8] JIA Zhi-hong, DING Li-peng, WENG Yao-yao, WEN Zhang, LIU Qing. Effects of high temperature pre-straining on natural aging and bake hardening response of Al−Mg−Si alloys [J]. Transactions of Nonferrous Metals Society of China, 2016, 26: 924−929.

[9] YANG Qun-ying, YANG Dong, ZHANG Zhi-qing, CAO Ling-fei, WU Xiao-dong, HUANG Guang-jie, LIU Qing. Flow behavior and microstructure evolution of 6A82 aluminum alloy with high copper content during hot compression deformation at elevated temperatures [J]. Transactions of Nonferrous Metals Society of China, 2016, 26: 649−657.

[10] ROBSON J D, PRANGNELL P B. Dispersoid precipitation and process modeling commercial aluminium alloys [J]. Acta Materialia, 2001, 49(4): 599−613.

[11] CONG Fu-guan, ZHAO Gang, JIANG Feng, TIAN Ni, LI Rui-feng. Effect of homogenization treatment on microstructure and mechanical properties of DC cast 7X50 aluminum alloy [J]. Transactions of Nonferrous Metals Society of China, 2015, 25: 1027−1034.

[12] ZHAO Zhi-hao, CUI Jian-zhong, DONG Jie, ZHANG Bei-jiang. Effect of low frequency magnetic field on microstructures and macrosegregation of horizontal direct chill casting 7075 aluminum alloy [J]. Journal of Materials Processing Technology, 2007, 182(1−3): 185−190.

[13] RANGANATHAR R, KUMAR V A, NNAND V S, NURALIDHARA B K. Multi-stage heat treatment of aluminum alloy AA7049 [J]. Transactions of Nonferrous Metals Society of China, 2013, 23: 1570−1575.

[14] LI X M, STARINK M J. The effect of compositional variations on characteristics of coarse intermetallic particles in overaged 7000 aluminum alloys [J]. Materials Science and Technology, 2001, 17(11): 1324−1328.

[15] FAN Xi-gang, JIANG Da-ming, MENG Qing-chang, LI Zhong. The microstructural evolution of an Al−Zn−Mg−Cu alloy during homogenization [J]. Materials Letters, 2006, 60(12): 1475−1479.
[16] DENG Ying, YIN Zhi-min, CONG Fu-guan. Intermetallic phase evolution of 7050 aluminum alloy during homogenization [J]. Intermetallics, 2012, 26(7): 114−121.
[17] HE Li-zi, LI Xie-hua, ZHU Pei, CAO Yi-heng, GUO Ya-ping, CUI Jian-zhong. Effects of high magnetic field on the evolutions of constituent phases in 7085 aluminum alloy during homogenization [J]. Materials Characterization, 2012, 71(9): 19−23.
[18] MONDAL C, MUKHOPADHYAY A K. On the nature of $T(Al_2Mg_3Zn_3)$ and $S(Al_2CuMg)$ phases present in as-cast and annealed 7055 aluminum alloy [J]. Materials Science and Engineering A, 2005, 391(1−2): 367−376.
[19] YAN Li-zhen, ZHANG Yong-an, LI Xi-wu, LI Zhi-hui, WANG Feng, LIU Hong-wei, XIONG Bai-qing. Microstructural evolution of Al−0.66Mg−0.85Si alloy during homogenization [J]. Transactions of Nonferrous Metals Society of China, 2014, 24: 939−945.
[20] WU Yue-mei, XIONG Ji, LAI Ren-ming, ZHANG Xian-yu, GUO Zhi-xing. The microstructure evolution of an Al−Mg−Si−Mn−Cu−Ce alloy during homogenization [J]. Journal of Alloys and Compounds, 2009, 475(1−2): 332−338.
[21] BIROL Y. The effect of homogenization practice on the microstructure of AA6063 billets [J]. Journal of Materials Processing Technology, 2004, 148(2): 250−258.
[22] CAI M, ROBSON J, LORIMER G W, PARSON N C. Simulation of the casting and homogenization of two 6xxx series alloy [J]. Materials Science Forum, 2002, 396−402: 209−214.
[23] JI Yan-li, GUO Fu-an, PAN Yan-feng. Microstructural characteristics and paint-bake response of Al−Mg−Si−Cu alloy [J]. Transactions of Nonferrous Metals Society of China, 2008, 18: 126−131.
[24] MARGARITA S, MILOS J, MIROSLAV C. Effect of low temperature stabilisation on the precipitation of a continuously cast Al–Mg–Si alloy [J]. Materials Science and Engineering A, 2007, 462: 375–379.
[25] ROBSON J D. Microstructural evolution in aluminium alloy 7050 during processing [J]. Materials Science and Engineering A, 2004, 382: 112−121.
[26] GODARD D, ARCHAMBAULT P, AEBYGAUTIER E, LAPASSET G. Precipitation sequences during quenching of the AA7010 alloy [J]. Acta Materialia, 2002, 50: 2319−2329.
[27] LI Y Y, ZHANG W W, FEI J, ZHANG D T, CHEN W P. Heat treatment of 2024/3003 gradient composite and diffusion behavior of the alloying elements [J]. Materials Science and Engineering A, 2005, 391: 124−130.
[28] WANG Tong-min, LIANG Chun-hui, CHEN Zong-ning, ZHENG Yuan-ping, KANG Hui-jun, WANG Wei. Development of an 8090/3003 bimetal slab using a modified direct-chill casting process [J]. Journal of Materials Processing Technology, 2014, 214: 1806−1811.
[29] CONSERVA M, DI RUSSO E, CALONI O. Comparison of the influence of chromium and zirconium on the quench sensitivity of Al−Zn−Mg−Cu alloys [J]. Metallurgical Transactions, 1971, 2: 1227−1232.
[30] THOMPSON D S, SUBRAMANYA B S, LEVY S A. Quench rate effects in Al−Zn−Mg−Cu alloys [J]. Metallurgical Transactions, 1971, 2: 1149−1160.

均匀化退火对 7050/6009 复层板坯组织、成分和力学性能的影响

闫光远[1]，毛 丰[1]，陈 飞[1]，曹志强[2]，王同敏[1]

1. 大连理工大学 材料科学与工程学院 三束材料改性教育部重点实验室，大连 116024；
2. 大连理工大学 原材料特种制备技术实验室，大连 116024

摘 要：研究均匀化退火对直接冷却法制备的 7050/6009 复层板坯界面区域的组织演化、成分分布和力学性能的影响。结果表明，最佳的均匀化退火工艺是 460 °C 条件下保温 24 h。均匀化退火后，在复层板坯界面处沉淀出了富锌相和 $Al_{15}(FeMn)_3Si_2$ 相。均匀化时间固定为 24 h 的条件下，当均匀化温度由 440 °C 增加到 480 °C 时，复层试样的扩散层厚度增加了 30 μm；均匀化温度固定为 460 °C 条件下，当均匀化时间由 12 h 增加到 36 h 时，复层试样的扩散层厚度增加了 280 μm。均匀化退火后，复层合金的 6009 合金侧和界面处的维式硬度均降低，晶粒粗化为主要的软化机制；然而 7050 合金侧的维式硬度变化较复杂，原因归结为固溶强化、弥散强化和增强相的溶解的混合作用。

关键词：复层板坯；均匀化退火；组织；扩散层；力学性能

(Edited by Yun-bin HE)